Ground deformation due to magma ascent with and without degassing

doi: 10.1029/2006GL028101

Ground deformation due to magma ascent with and without degassing

Takeshi Nishimura[1]

Received 7 September 2006; revised 1 November 2006; accepted 9 November 2006; published 13 December 2006.

[1] I numerically calculate upward migration of vesiculated magma in an elastic volcanic conduit, taking into account the bubble growth in melt, elastic stress from the surrounding medium, and degassing from the magma. The results show that when magma containing gas bubbles reaches the ground surface without degassing, the ground deformation accelerates just before the eruption in response to volumetric expansion of the magma. On the other hand, the rate of change in ground deformation is almost constant when the magma degasses as it ascends. Similar characteristics have been observed in ground deformation recorded before explosive eruptions and lava extrusion at several active volcanoes. These consistencies strongly suggest that geodetic measurements, which have been mainly used to date to estimate the eruption time and the locations of magmatic intrusions, provide a basis for predicting the volcanic explosivity and monitoring bubble growth and degassing processes in the conduit. **Citation:** Nishimura, T. (2006), Ground deformation due to magma ascent with and without degassing, *Geophys. Res. Lett.*, *33*, L23309, doi:10.1029/2006GL028101.

1. Introduction

[2] Volcanic explosive eruptions rapidly eject hot volcanic ash and gasses from the vent into the atmosphere, occasionally generating dangerous pyroclastic flows that propagate down the flanks of volcanoes at high speed. Such volcanic flows often severely damage human infrastructure surrounding the volcano. On the other hand, lava dome eruptions slowly extrude viscous lava from the vent, and are relatively benign. Although pyroclastic flows sometimes occur following lava dome collapse, there is generally more time to prepare for the disaster beforehand, since the lava dome formation precedes the pyroclastic flow. These two types of eruptions are much different, but both can be observed during a single sequence of volcanic eruptions, as has happened at Mount St. Helens, Unzen and elsewhere [*Swanson et al.*, 1983; *Nakada et al.*, 1999].

[3] It is well known that volcanic explosions are mainly excited by gas bubbles in melt, and that sufficient loss of that gas during magma ascent can reduce the possibility of an explosive eruption occurring. Numerous analyses of geologic samples [e.g., *Rust and Cashman*, 2004; *Takeuchi et al.*, 2005], laboratory experiments, and theoretical investigations [*Proussevitch et al.*, 1993; *Proussevitch and Sahagian*, 1996; *Lyakhovsky et al.*, 1996; *Lensky et al.*, 2004] have been carried out to elucidate the dynamics of gas bubbles and mechanisms of degassing during the last several decades. Magmas residing in deep magma chambers contain appreciable amounts of volatiles in melt [*Taylor et al.*, 1983]. Numerous gas bubbles form within a magma as the volatiles begin to saturate it as it ascends [*Toramaru*, 1989; *Yamada et al.*, 2005]. If the magma, which consists of gas bubbles and melt in the conduit, loses most of the gases (by permeable or diffusive flow, for instance) before it reaches the ground surface, lava dome formation occurs [*Eichelberger et al.*, 1986]. Otherwise, the gas bubbles dramatically expand in volume as the magma ascends, until the magma is ultimately fragmented and a violent volcanic explosive eruption occurs.

[4] These studies suggest that the measurement of degassing from magma body is important for understanding the volcanic explosivity. However, direct measurements of volcanic gasses have been difficult to undertake, mainly because there are many pathways of degassing, contact between ascending magma and shallow ground water and so on. Recently, bubble growth processes have been theoretically linked to deformation of the surrounding elastic medium [*Chouet et al.*, 2006; *Nishimura*, 2004; *Shimomura et al.*, 2006], and bubble growth in a deep magma chamber has been detected with strain meters at Soufriere Hills on Montserrat volcano [*Voight et al.*, 2006]. In the present study, therefore, I examine ground deformation for two cases of magma ascent by simply modeling the degassing process. The first is magma ascent without degassing, during which the gas bubbles are conserved in the melt until it reaches the ground surface. The second is magma ascent with progressive degassing, in which gas bubbles or volatiles are progressively lost as the magma ascends to shallow depths.

2. Magma Ascent Model

[5] Magma ascent without degassing is modeled as follows. Magma is presumed to be initially at rest in the conduit beneath a magmatic lid, being balanced by lithostatic pressure from the top to the bottom (Figure 1a). The magma comprises compressible melt and numerous small gas bubbles assumed to be uniformly packed [*Proussevitch et al.*, 1993]. The gas bubbles, which have a same radius, and melt are assumed to be in equilibrium before the magma ascends. When additional magma is supplied to the system from below or a small pressure increase occurs, the lid opens and the magma starts to migrate upward in response to buoyancy forces stemming from the difference in density between the surrounding rocks and the magma.

[6] For the calculations, the magma is divided into n elements in the vertical direction: Figure 1b shows the grid points at which pressure and density of magma are computed, and the boundaries between adjacent fluid elements. U is the displacement, a dot represents the time derivative, P is the pressure, and ρ the magma density. A subscript, i, indicates

[1]Department of Geophysics, Graduate School of Science, Tohoku University, Sendai, Japan.

0094-8276/06/2006GL028101$05.00

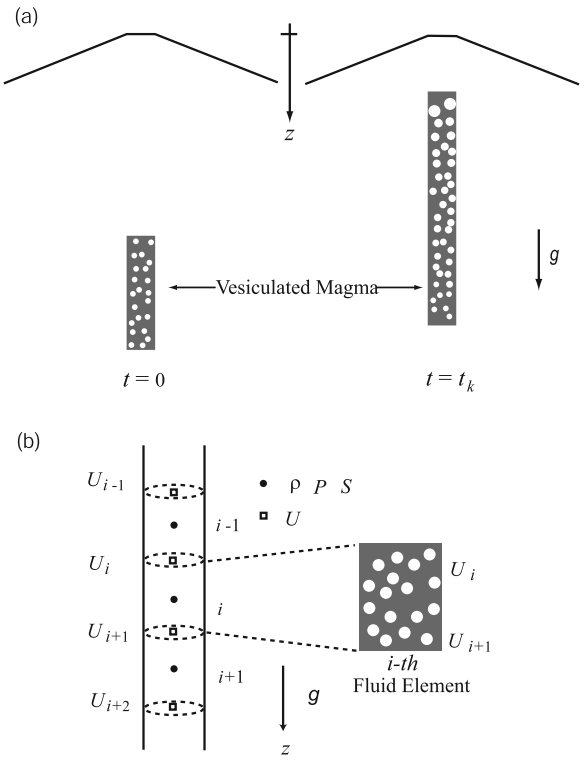

Figure 1. (a) Schematic illustration of magma ascending without degassing. (b) Grids of pressure, density and fluid element boundaries employed for the finite-difference calculations.

the number of each element. The vertical movement of each element is calculated with a finite difference method using a Lagrangian description of one-dimensional flow so that the vertical extension (or contraction) of each element is determined by the equation of motion: the displacement of the i-th element at time $t + \Delta t$ is calculated from the pressure and velocity at time t:

$$\frac{\dot{U}_i^{t+\Delta t} - \dot{U}_i^t}{\Delta t} = -\frac{2\left(P_i^t - P_{i-1}^t\right)}{\overline{\rho}_i^t\left(U_{i+1}^t - U_{i-1}^t\right)} - g - \frac{12\eta\dot{U}_i^t}{\overline{\rho}_i^t d^2}, \qquad (1)$$

where $\overline{\rho}_i^t$ is the average density of elements $i-1$ and i, η the viscosity of magma and d the conduit width. At the same time, bubble growth is calculated using the formula of *Proussevitch et al.* [1993], the momentum equation of the melt, mass conservation of volatiles (H_2O), and a diffusive representation of volatile movement in the melt. In response to a small pressure decrease accompanying upwards movement during a small increment of time Δt, the bubble radius, volatile concentrations, magma density and so on are calculated at time $t + \Delta t$ under a condition of no strain from the surrounding elastics [*Nishimura*, 2004]. It is supposed that no new bubble is created, the system is under isothermal condition, and magma properties such as viscosity, surface tension, diffusivity coefficient and so on are constant during the magma ascent and bubble growth [*Shimomura et al.*, 2006]. These equations are independently solved for each element.

[7] Since the mass of the magma must always be conserved in each element, horizontal strain is necessary when the vertical extension alone cannot completely account for the total volume changes due to any bubble growth. The mass conservation for each element is expressed by:

$$\rho_i^t S_i^t\left(U_{i+1}^t - U_i^t\right) = m_i, \qquad (2)$$

where S_i^t is the cross-sectional area of the i-th element at time t and m_i the mass of the element. Horizontal displacements are estimated by substituting the density and displacement of the top and bottom of each element, into equation (2). The resulting stress applied by the surrounding elastic medium is added to the melt pressure within each element [*Nishimura*, 2004; *Shimomura et al.*, 2006]. By repeating these steps, the interactions between gas bubbles, melt and the surrounding medium are coupled with each other. The top of the magma column is assumed to remain subjected to lithostatic pressure, in order to control its vertical propagation. This simple treatment, in which no additional force is necessary to open the conduit, is likely to be generally applicable when magma migrates along a preexisting path or the crack stiffness at the top of column is very low.

[8] In the case of magma ascent with degassing, I suppose that magma first migrates upward in the same way as during magma ascent without degassing. When the magma reaches a shallow depth z_d, bubble growth ceases and degassing begins. The degassing process is modeled by constantly increasing the magma density:

$$\rho_i^{t+\Delta t} = (1 + \alpha\Delta t)\rho_i^t, \qquad (3)$$

The coefficient α controls the rate of degassing, which is considered to be with a function of the volume and/or surface area of the magma, the void ratio, permeability and other magma properties. It is assumed that the degassed gasses immediately part from the magma and do not affect the magma motion.

3. Results of Numerical Calculations

[9] Figure 2a shows an example of spatiotemporal variations in an ascending magma without degassing. Magma body is initially located at depths of 5–7 km with a conduit width of 5 m and an aspect ratio of 0.1 (that is, the cross-section of the magma column forms an elliptical shape with major and minor axes of 50 m and 5 m, respectively). Magma properties corresponding to a rhyolite are used (Table 1). The calculations are performed by dividing the magma into 40 vertically juxtaposed elements, and stopped when the top of magma reaches a depth of 50 m.

[10] Magma begins to migrate upwards, and soon reaches a migration speed of about 0.06 m/s, which is determined by the balance between the buoyancy force and viscous drag from the conduit wall. Since the initial melt pressures are different at each depth, bubble growth in the upper parts progresses faster than lower in the magma volume [*Shimomura et al.*, 2006]. As a result, the upper parts attain greater buoyancy and vertically elongate the magma: when the magma reaches a depth of 50 m, the magma body's length is about 3.8 km, nearly twice the original value. Horizontal extension is observed until the top of magma reaches about 4 km depth. This extension is explained in terms of the

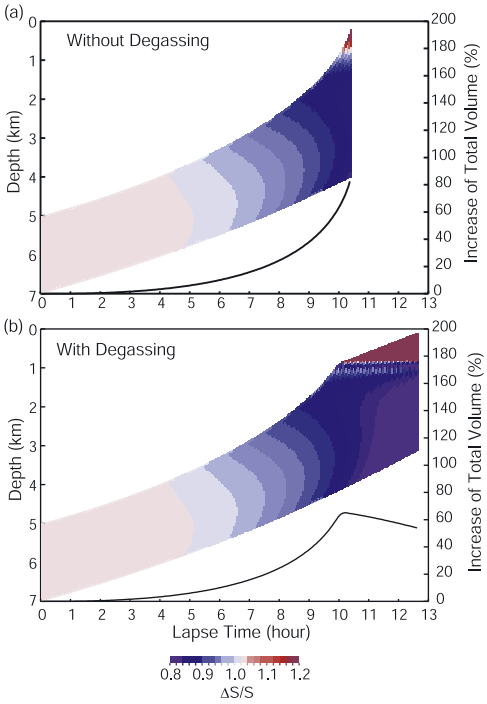

Figure 2. Spatiotemporal variations in the cross-sectional area of the magma conduit for magma ascent (a) without degassing and (b) with degassing. Red and blue colours represent inflation and deflation of each element from the initial cross-sectional area, respectively. In the case of (b), the degassing starts at a depth of 1 km and α is assumed to be constant (0.0008 s^{-1}). The other model parameters are same in (a) and (b).

pressure recovery of melt subjected to a pressure drop during upward migration. After that point, the volcanic conduit starts to deflate in response to vertical extension of the magma column as well as weak pressure recovery for a given large pressure drop [*Nishimura*, 2004]. The changes in horizontal extension and contraction are mostly within the range of a few percent, and a few tens of percent at maximum. As a result, the magma volume increases to 180% of the initial volume just before it reaches the ground surface.

[11] Figure 2b shows an example of the magma ascent with degassing for z_d = 1 km and α = 0.0008 s^{-1}. The magma volume initially increases with progressive shallowing, as is the case without degassing. However, once the magma begins to degas at a depth of 1 km, the volume gradually decreases and the upward migration velocities of the upper part of the magma body become constant.

[12] Figure 3 compares the ground deformation produced by ascending magma with and without degassing. The calculation assumes a semi-infinite homogeneous space and tensile crack opening for simplicity [*Okada*, 1992]. The ground displacements due to the magma rising without degassing accelerate rapidly (Figure 3a). Due to volumetric expansion and the increase in upward velocity of the magma, the curves shown are concave in shape and the displacement rapidly increases as the magma nears the ground surface. In the case of magma ascending with degassing starting at z_d = 1 km (Figure 3b), the displacement increases with time, but the rate of the change (i.e., velocity) remain almost constant: this effect is caused mainly by the decrease of magma volume with degassing. In the case of z_d = 5 km (Figure 3c), the rate of the change is larger than in the case of z_d = 1 km but much smaller than in the case without degassing, because the magma volume is preserved and the migration speed remains constant.

4. Discussion

[13] Ground deformation records associated with explosive volcanic eruptions and lava dome formations have been reported at several active volcanoes. For example, during the 1981 volcanic activity at Mount St. Helens, records from a tilt meter installed near the lava dome [*Dzurizin et al.*, 1999] showed rapid changes just before a moderate-sized explosion on March 19, while constant rate of tilt changes were observed for lava dome formation on April 5. Tilt records at Merapi volcano show a high rate change before the 1997 and 1998 eruptions that show explosivity [*Voight et al.*, 2000]. This is in contrast to the steady inflations observed before the eruptions of nuée ardente (pyroclastic flows) generated by gravitational dome-collapse in 1994, 1995 and 1996. Before the initial lava dome formations during the mid-May 1991 crisis at Unzen volcano [*Yamashina and Shimizu*, 1999; *Saito et al.*, 1993] and the September 1995 Soufriere Hills activity at Montserrat volcano [*Jackson et al.*, 1998], horizontal distance changes or tilt motion at a constant rate were detected by geodetic measurements. There are not many examples observed until now, but these four volcanoes agree with the prediction from magma ascent models with and without degassing. However, the 1997 first lava extrusion at Colima volcano showed an accelerated decrease in slope distance [*Ramírez-Ruiz et al.*, 2002]. This case may not fit with the magma ascent models, but the inconsistency may be related with a very long duration of the changes (about 1 year) or sparse sampling of the data.

[14] Volumetric expansion is inherent in ascending magmas that retain numerous gas bubbles, whereas degassing inevitably reduces the magma volume in an elastic conduit. Therefore, irrespective of what the mechanisms of degassing are, ground deformation measurements can potentially detect the difference between magmas producing explosive eruptions and those forming lava domes. High quality data of geodetic measurements made using GPS, tilt and strain meters, and InSAR — which have been mainly used to date to estimate the eruption time and the locations of magmatic intrusions [e.g., *Kamo and Ishihara*, 1989; *Miura et al.*, 2000; *Fukushima et al.*, 2005; *Sato and Hamaguchi*, 2006]— may prove useful for predicting the volcanic explosivity, and

Table 1. Parameters of Rhyolite Magma and Surrounding Elastic Medium

Parameter	Value
Diffusivity coefficient	10^{-11} m^2s^{-1}
Viscosity	10^5 Pa s
Henry constant	1.6×10^{-11} Pa^{-1},
Surface tension	0.2 N m^{-1}
Melt density	2200 kg m^{-3}
Bulk modulus of melt	1.38×10^{10} Pa.
Temperature of magma	1300 K
Molecular weight of water	0.018 kg mol^{-1}
Gas constant	8.31 J $K^{-1}mol^{-1}$
Rigidity of the surrounding elastic medium	1.1×10^{10} Pa
Poisson's ratio of the surrounding elastic medium	0.25

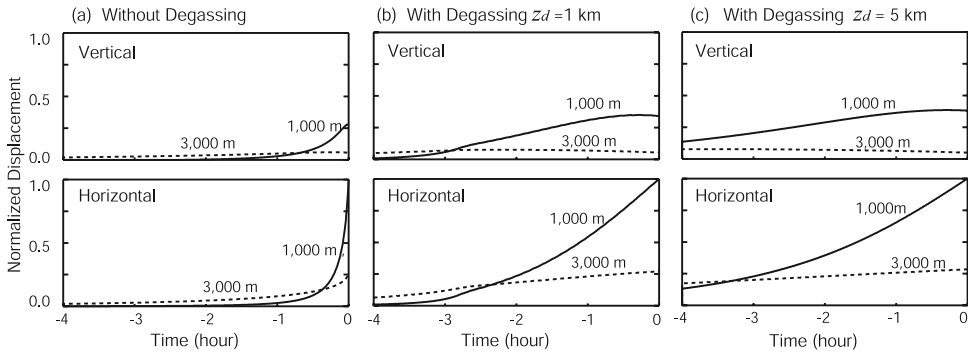

Figure 3. Vertical and horizontal displacements caused by magma ascending (a) without degassing, (b) with degassing from 1 km, and (c) with degassing from 5 km. The thick and dotted lines represent displacements at 1000 m and 3000 m from the vent, respectively. Displacements are normalized by the maximum horizontal displacements at 1000 m in each case. The horizontal axis represents the time in hours relative to the time at which the magma reaches a depth of 50 m.

further improvement of magma ascent processes in volcanic edifice with more comprehensive magma properties (e.g., viscosity dependent on the volatile contents) will enable us to more accurately evaluate the bubble growth and degassing processes in the conduit.

[15] **Acknowledgments.** This study was partly supported by a Grant for Scientific Research from MEXT (14080202). Helpful comments by Oleg Melnik and Peter Cervelli improved the manuscript.

References

Chouet, B. A., P. Dawson, and M. Nakano (2006), Dynamics of diffusive bubble growth and pressure recovery in a bubbly rhyolitic melt embedded in an elastic solid, *J. Geophys. Res.*, *111*, B07310, doi:10.1029/2005JB004174.

Dzurizin, D., J. A. Westphal, and D. J. Johnson (1999), Eruption prediction aided by electronic tiltmeter data at Mount St. Helens, *Science*, *221*, 1381–1383.

Eichelberger, J. C., C. R. Carrigan, H. R. Westrich, and R. H. Price (1986), Non-explosive silicic volcanism, *Nature*, *323*, 598–602.

Fukushima, Y., V. Cayol, and P. Durand (2005), Finding realistic dike models from interferometric synthetic aperture radar data: The February 2000 eruption at Piton de la Fournaise, *J. Geophys. Res.*, *110*, B03206, doi:10.1029/2004JB003268.

Jackson, P., et al. (1998), Ground deformation studies at Soufriere Hills Volcano, Montserrat: I. Electronic distance meter studies, *Geophys. Res. Lett.*, *25*, 3409–3412.

Kamo, K., and K. Ishihara (1989), A preliminary experiment on automated judgment of the stages of eruptive activity using tiltmeter records at Sakurajima, Japan, in *Volcanic Hazards: Assessment and Monitoring—IAVCEI Proceedings in Volcanology*, edited by J. H. Latter, pp. 585–598, Springer, New York.

Lensky, N. G., O. Navon, and V. Lyakhovsky (2004), Bubble growth during decompression of magma: Experimental and theoretical investigation, *J. Volcanol. Geotherm. Res.*, *129*, 7–22.

Lyakhovsky, V., S. Hurwitz, and O. Navon (1996), Bubble growth in rhyolitic melts: Experimental and numerical investigation, *Bull Volcanol.*, *58*, 19–32.

Miura, S., S. Ueki, T. Sato, K. Tachibana, and H. Hamaguchi (2000), Crustal deformation associated with the 1998 seismo-volcanic crisis of Iwate Volcano, Northeastern Japan, as observed by a dense GPS network, *Earth Planets Space*, *52*, 1003–1008.

Nakada, S., H. Shimizu, and K. Ohta (1999), Overview of the 1990–1995 eruption at Unzen volcano, *J. Volcanol. Geotherm. Res.*, *89*, 1–22.

Nishimura, T. (2004), Pressure recovery in magma due to bubble growth, *Geophys. Res. Lett.*, *31*, L12613, doi:10.1029/2004GL019810.

Okada, Y. (1992), Internal deformation due to shea and tensile faults in a half-space, *Bull. Seismol. Soc. Am.*, *82*, 1018–1040.

Proussevitch, A., and D. L. Sahagian (1996), Dynamics of coupled diffusive and decompressive bubble growth in magmatic systems, *J. Geophys. Res.*, *101*, 17,447–17,456.

Proussevitch, A., D. L. Sahagian, and A. T. Anderson (1993), Dynamics of diffusive bubble growth in magmas: Isothermal case, *J. Geophys. Res.*, *98*, 22,283–22,307.

Ramírez-Ruiz, J. J., H. Santiago-Jiménez, E. Alatorre-Chávez, and M. Bretón-González (2002), EDM deformation monitoring of the 1977–2000 activity at Volcán de Colima, *J. Volcanol. Geotherm. Res.*, *117*, 61–67.

Rust, A. C., and K. V. Cashman (2004), Permeability of vesicular silicic magma: Inertial and hysteresis effects, *Earth Planet Sci. Lett.*, *228*, 93–107.

Saito, E., et al. (1993), Geodetic monitoring using EDM before and during the 1991–1992 lava extrusion of Fugen-dake, Unzen Volcano, Kyushu, Japan (in Japanese with English abstract), *Bull. Geol. Surv. Jpn.*, *44*, 639–647.

Sato, M., and H. Hamaguchi (2006), Weak long-lived ground deformation related to Iwate volcanism revealed by Bayesian decomposition of strain, tilt and positioning data, *J. Volcanol. Geotherm. Res.*, *155*, 244–262.

Shimomura, Y., T. Nishimura, and H. Sato (2006), Bubble growth processes in magma surrounded by an elastic medium, *J. Volcanol. Geotherm. Res.*, *155*, 307–322.

Swanson, D. R., et al. (1983), Predicting eruptions at Mount St. Helens, June 1980 through December 1982, *Science*, *221*, 1369–1375.

Takeuchi, S., S. Nakashima, A. Tomiya, and H. Shinohara (2005), Experimental constraints on the low gas permeability of vesicular magma during decompression, *Geophys. Res. Lett.*, *32*, L10312, doi:10.1029/2005GL022491.

Taylor, B. E., J. C. Eichelberger, and H. R. Westrich (1983), Hydrogen isotopic evidence for rhyolitic magma degassing during shallow intrusion and eruption, *Nature*, *306*, 541–545.

Toramaru, A. (1989), Vesiculation process and bubble size distribution in ascending magma with constant velocities, *J. Geophys. Res.*, *94*, 17,523–17,542.

Voight, B., et al. (2000), Deformation and seismic precursors to dome-collapse and fountain-collapse nuées ardentes at Merapi Volcano, Java, Indonesia, 1994–1998, *J. Volcanol. Geotherm. Res.*, *100*, 261–287.

Voight, B., et al. (2006), Unprecedented pressure increases in deep magma reservoir triggered by lava-dome collapse, *Geophys. Res. Lett.*, *33*, L03312, doi:10.1029/2005GL024870.

Yamada, K., H. Tanaka, K. Nakazawa, and H. Emori (2005), A new theory of bubble formation in magma, *J. Geophys. Res.*, *110*, B02203, doi:10.1029/2004JB003113.

Yamashina, K., and H. Shimizu (1999), Crustal deformation in the mid-May 1991 crisis preceding the extrusion of a dacite lava dome at Unzen volcano, Japan, *J. Volcanol. Geotherm. Res.*, *89*, 43–55.

T. Nishimura, Department of Geophysics, Graduate School of Science, Tohoku University, Aramaki-aza Aoba 6-3, Aoba-ku, Sendai 980-8578, Japan. (nishi@zisin.geophys.tohoku.ac.jp)